THE JOURNAL OF BIOLOGICAL CHEMISTRY VOL. 281, NO. 39, pp. 29148–29154, September 29, 2006

Insights into Allosteric Control of Vinculin Function from Its Large Scale Conformational Dynamics*

Received for publication, June 8, 2006 Published, JBC Papers in Press, August 6, 2006, DOI 10.1074/jbc.M605512200

Yiwen Chen[‡] **and Nikolay V. Dokholyan**[§1]

From the [‡]*Department of Physics and Astronomy and the* [§]*Department of Biochemistry and Biophysics, University of North Carolina, Chapel Hill, North Carolina 27599*

Vinculin is an important constituent of both cell-cell and cell-matrix junctions, where it plays crucial roles in the regulation of cell adhesion and migration. When activated, it mediates the linkage between cadherins (cell-cell) or integrins (cell-matrix) and the actin cytoskeleton through interactions with various proteins. The activation of vinculin requires structural conversions from an autoinhibited conformation to the "open" conformations in which the occluded binding sites of its different ligands become exposed, while the structural dynamics underlying the vinculin activation remains largely unknown. Here we report the first computational study of large scale conformational dynamics of full-length vinculin. We find that the "holding" and "releasing" motions between vinculin tail and pincer-like structure formed by first three domains of vinculin are the dominant motions near the native state of vinculin, indicating that an inherent flexibility of vinculin has a large influence on its allostery. We also find a cooperative dissociation between the head and tail domains of vinculin with increasing temperature in both thermodynamic and kinetic simulations, implying that vinculin may function as an allosteric switch in response to external signals. We show that the kinetics of vinculin unfolding exhibits specific sequential patterns, suggesting that a sophisticated interplay between domains may synergistically contribute to vinculin activation. We further find that the interaction between vinculin-binding site peptide from talin and vinculin significantly destabilizes the intramolecular head-tail interactions, suggesting a direct role of talin binding in vinculin activation.

Vinculin, a highly conserved 117-kDa intracellular protein (1066 residues), plays critical roles in the maintenance and regulation of cell shape, adhesion, and migration (1–5) that are essential to many physiological and pathological processes such as embryogenesis, wound healing, and metastasis. In its inactive state, vinculin is held in a "closed," autoinhibited conformation by intramolecular interactions between the head and tail domains (Vt) (6, 7). Upon recruitment to cell-cell and cell-matrix junctions, vinculin becomes activated and provides a structural link between the membrane and actin filaments in both locales (8–10), although the exact role of vinculin in the formation of adhesion complexes is unknown.

The crystal structure of vinculin is composed of a series of helix bundles that are arranged into five distinct domains (11) (*D1–D5*, Fig. 1). Each of the first three domains (D1–D3) comprises two four-helix bundles that share a central long α-helix, whereas D4 is a single four-helix bundle that is connected to Vt (D5) by a proline-rich linker region (Fig. 1). Domains D1 and D3 form a pincer-like structure holding the vinculin tail in an autoinhibited state (Fig. 1) in which many ligand-binding sites are occluded. Domain D2 stabilizes the pincer-like structure by forming extensive contacts with domain D3.

The activation of vinculin requires the release of the interaction between the D1 (residue 1–258) and Vt (residue 896–1066) domains, which is triggered by binding to different ligands. Early biochemical and structural studies established the role of an acidic phospholipid PtdIns(4,5)P_2[2] in disrupting the interaction between D1 and Vt by binding to Vt domain (12–14). The release of the D1-Vt interaction further exposes cryptic binding sites in vinculin for other ligands, including talin, α-actinin, α-catenin, vasodilator-stimulated phosphoprotein (VASP), vinexin, ponsin, actin-related protein complex (Arp2/3), paxillin, and actin (9). In contrast, the role of talin in releasing the head-tail interaction was uncovered more recently (15, 16). It was found that the binding of specific short talin peptides (~30 amino acids) to the D1 domain alone is sufficient for releasing intramolecular head-tail interactions in the D1-Vt complex by provoking significant structural changes of the D1 domain, suggesting an alternative pathway of vinculin activation, in which PtdIns(4,5)P_2 may not be required (15, 16). However, Bakolitsa *et al.* (11) and Gilmore and Burridge (12) demonstrated that larger fragments of talin bind poorly to full-length vinculin *in vitro*. When PtdIns(4,5)P_2 is added, binding strength increases 4-fold (12). Hence it is more likely that the activation of vinculin is achieved by a combinatorial binding of ligands rather than any single ligand (11, 17).

Despite intensive biophysical and biochemical studies, a global and dynamic picture of vinculin activation is still lacking. Experimental characterization of the large scale conformational dynamics relevant to vinculin activation is challenging. Even using computational methods, the time scale of the conformational dynamics and the size of vinculin are beyond the resolution capabilities of the current all-atom molecular

* This work was supported in part by Muscular Dystrophy Association Grant MDA3720, American Heart Association Grant 0665361U, and North Carolina Biotechnology Center Grant 2006-MRG-1107 (to N. V. D.). The costs of publication of this article were defrayed in part by the payment of page charges. This article must therefore be hereby marked "*advertisement*" in accordance with 18 U.S.C. Section 1734 solely to indicate this fact.

[1] To whom correspondence should be addressed: Dept. of Biochemistry and Biophysics, University of North Carolina, Chapel Hill, NC 27599. Tel.: 919-843-2513; Fax: 919-966-2852; E-mail: dokh@med.unc.edu.

[2] The abbreviations used are: PtdIns(4,5)P_2, phosphatidylinositol 4,5-bisphosphate; DMD, discrete molecular dynamics; PDB, Protein Data Bank.

dynamics simulation techniques. Hence, to uncover the large scale conformational dynamics associated with vinculin function, we utilize rapid discrete molecular dynamics (DMD) (18–20) techniques. We find distinct and complementary roles of internal (inherent flexibility, domain-domain interactions within vinculin) and external (talin binding) factors in allosteric control of vinculin, suggesting possible mechanisms for vinculin activation.

MATERIALS AND METHODS

Homology Modeling of Missing Loop Structure—The conformation of a loop (856–874) is missing in the x-ray structure of vinculin. We used the biopolymer module of the program SYBYL to reconstruct the backbone conformation of this loop. The reconstruction is based on homology modeling method (21). By searching the structural homologues of this loop in the Brookhaven Protein Data Bank (PDB) (22), we used SYBYL to generate a candidate list of loop structures for reconstruction. From this list as the template for reconstruction we chose the loop structure (PDB accession code: 1KZQ, chain B, residues 191–212) that has the highest sequence identity (26.1%) to the missing loop. We further used SYBYL to integrate the reconstructed loop conformation into the original vinculin structure. We further added side chains to amino acids on the reconstructed backbone. We determined the optimal rotamer states of side chains by a Monte-Carlo minimization procedure (23).

Protein and Interaction Model—We performed DMD simulations using a simplified two-bead protein model, in which each residue was represented by one backbone bead C_α and one side chain bead C_β (only C_α for Gly). The detailed implementation of covalent bonds and constraints that maintain the geometry of each residue in the model can be found in Ref. 24. In addition to the covalent bonds and constraints, we used the Gō potential (25, 26) to model the non-bonded interactions within monomers. The chicken vinculin crystal structure (11) (PDB accession code 1ST6) with reconstructed loop was used as native structure to assign the Gō potential. We also incorporated backbone hydrogen bonding interaction into the simulations (27).

Thermodynamic and Kinetic Simulations—In thermodynamic studies, prior to the equilibrium simulations we performed simulations for 1×10^5 time units from the initial temperature $T = 0.1$ to various target temperatures in the range between $T = 0.1$ and $T = 2.0$ (simulation temperature is in units of ϵ/k_B, where ϵ is the energy unit and k_B is Boltzmann's constant). We then performed equilibrium simulations for 1×10^6 time units at the corresponding target temperatures. In kinetic studies, we performed 20 unfolding simulations starting from the same native structure of vinculin but different initial velocities. In each kinetic unfolding simulation, we gradually (during 5×10^5 time unit) increased the system temperature from $T = 0.1$ to $T = 0.9$. We then analyzed the pattern of dissociations between domains and within domains during the course of unfolding.

Fraction of Native Contacts as a Measure of Dissociation Magnitude—A native contact is defined to exist in a given conformation if the C_β atoms of two residues are within a cutoff distance (7.5 Å) both in this conformation and in the native structure. The cutoff distance used to define the native contact was the same as the one used to define structure-based Gō potential. The fraction of native contacts (Q) was defined as the ratio between the number native contacts in a given conformation and in the native structure. It takes the value ranging from one (when a protein adopts native structure) to zero (when a protein is fully unfolded) and has been used as a reaction coordinate in the study of protein folding (28).

Characterization of the Principal Motions Near the Native State—We used essential dynamics to characterize the principal motions near the native state. The essential dynamics (29, 30) were based on the diagonalization of the covariance matrix constructed from fluctuations of C_α atoms in the simulation trajectories in which the overall translation and rotation have been removed.

$$M = \langle (X_i - X_{i,0})(X_j - X_{j,0}) \rangle \qquad \text{(Eq. 1)}$$

X_i (X_j) in Equation 1 are the separate x, y, and z coordinates of the ith (jth) C_α atom ($i,j = 1 \ldots N$, N is the total number of C_α atoms) fluctuating around its average $X_{i,0}$. The average was taken over all the snapshots along the trajectories used for calculation. We used the trajectory from DMD simulation at low temperature ($T = 0.2$) where the native state was the most favorable state and protein undergoes conformational fluctuations near native state. The diagonalization of Equation 1 yields a set of eigenvectors (describing directions in the high dimensional configurational space) and eigenvalues (represent the mean square fluctuation of the total displacement along the eigenvectors). The first few eigenvectors with the highest eigenvalues describe principal motions. Motions along these eigenvectors are mainly large anharmonic fluctuations and generally can be linked to the biological functions of the proteins. The motions described by eigenvectors with small corresponding eigenvalues represent harmonic (Gaussian) fluctuations, which are thermal fluctuations in nature.

Simulation of the Interaction between Vinculin-binding Site Peptide from Talin and Vinculin—To investigate the role of talin binding in vinculin activation, we performed simulations of the binding of vinculin-binding site (VBS1, residue 605–636) from talin to vinculin. We modeled the interaction between vinculin and VBS1 by constructing the following effective potential,

$$\begin{aligned} E_{\text{tot}} &= E_{\text{vinculin-free}} + E_{\text{VBS1-free}} + E_{\text{interaction (vinculin-VBS1)}} \\ &= \sum_{i,j} \Delta_{i,j}^{\text{vinculin-free}} + \sum_{i,j} \Delta_{i,j}^{\text{VBS1-free}} \\ &\quad + \left(\alpha \sum_{i,j} \Delta_{i,j}^{\text{D1-bound}} + \sum_{i,j} \Delta_{i,j}^{\text{D1-VBS1}} \right) \end{aligned} \qquad \text{(Eq. 2)}$$

where $\{\Delta_{i,j}^{\text{vinculin-free}}\}$ and $\{\Delta_{i,j}^{\text{VBS1-free}}\}$ are the Gō-like pair-wise contact energies corresponding to the free state of vinculin (11) (PDB accession code 1ST6) and the free state of VBS1 (31) (PDB accession code 1SJ7), respectively. Matrices $\{\Delta_{i,j}^{\text{D1-bound}}\}$ and $\{\Delta_{i,j}^{\text{D1-VBS1}}\}$ are the Gō-like contact energies of the VBS1-bound state of D1 domain and between D1 domain and VBS1 that are assigned based on the D1-VBS1 complex structure (31) (PDB accession code 1TO1). The inclusion of contact energies for the

VBS1-bound state of D1 domain serves to effectively account for the conformational change of D1 upon VBS1 binding. For units that dissociate from each other, it is important to scale effective energy contribution to reflect the additional translational entropy gained by interacting domains. Parameter α is such scaling coefficient, the range of which is determined by consistency of simulations with experimental observations. More specifically, we determined the range of α by satisfying the following two conditions to be in agreement with experimental observations: first, without VBS1, the native state of the free D1 is the most stable state (root mean square from free D1 and VBS1-bound D1 structure are $<$2.4 and $>$3.0 Å, respectively); second, with VBS1, the experimentally determined D1-VBS1 complex is the most stable state at low temperatures (root mean square from complex structure is $<$2.4 Å). With the determined range of α was between 0.65 and 0.72, we then performed simulations in the presence of both VBS1 and vinculin at various temperatures. The simulation results are not sensitive to the exact value of α within the determined range. To improve the efficiency of simulation, we constrained the distance between C_β atoms of residue Ala^{616} of VBS1 peptide and residue Pro^{15} of D1 domain within 12 Å (these two atoms are within 7.5 in the native D1-Vt complex) so that the VBS1 and vinculin are spatially close to each other.

RESULTS

The Principal Motions Near the Native State—The principal motions that dominate conformational fluctuations in the vicinity of the native state of proteins often recapitulate the structural dynamics underlying their biological functions (32). To characterize the principal motions near the native state of vinculin, we first performed DMD simulations of vinculin at low temperature, where the native state of the protein is thermodynamically most favorable and the protein mainly undergoes small conformational fluctuations near its native state (see "Materials and Methods"). We then use essential dynamics analysis (29, 30) (see "Materials and Methods") to find the principal motions of the polypeptide chain. The first dominant mode is characterized by a breathing motion between two elements of vinculin structure (Fig. 1*a*). One such element consists of the end of the proline-rich linker region (Fig. 1) and the structural region from Vt helix bundle that is spatially proximal to the proline-rich linker region. The other element contains the structural region from D3 that is in spatial proximity to Vt and one of the two helix bundles from D2 that has extensive contacts with D3. The first dominant mode also involves a global twisting motion that occurs between two helix bundles within D2. The second dominant mode is highlighted by a holding and releasing motion between Vt domain and pincer-like structure formed by D1, D2 and D3 (Fig. 1*b*). The holding and releasing is synergized between the structural region from the Vt that is spatially proximal to D1, the structural region from D3 that is close to Vt and the middle region in the D2 structure (Fig. 1*b*). The third dominant mode involves the nearly parallel rotation and twisting of D1, D2, and Vt (Fig. 1*c*), reflecting the flexibility along the orthogonal directions distinct from the first two dominant modes. The interaction interface between D1 and Vt remains rigid in all three dominant modes of principal motions, indicating that the intramolecular interactions between D1 and Vt are kept intact under the conformational fluctuations near the native state.

The Thermal "Melting" of Intra- and Interdomain Interactions—To further characterize inter- and intradomain structural plasticities of vinculin that contribute to its function, we studied the thermal melting of inter- and intradomain interactions in vinculin. We performed equilibrium simulations at various system temperatures ranging from $T = 0.1$ to $T = 2.0$. At each temperature, we used the fraction of native contacts (see "Materials and Methods") to quantify the magnitude of dissociations between and within domains. We plotted the fractions of inter- and intradomain native contacts as functions of temperature (Fig. 2). We find that dissociations between most domains (D1-Vt, D3-D4, Vt-D3, D2-D3, Vt-D4, D1-D3) exhibit cooperative changes with increasing temperatures. In contrast, the association between D1 and D2 domain shows a gradual, rather than cooperative, decrease when temperature increases (Fig. 2*a*). In addition, we found that the associations between Vt and D3 domain were completely lost at the temperatures where the majority of the contacts between other domain pairs are kept, indicating that the effective interaction between the Vt-D3 pair was weaker compared with other pairs (Fig. 2*a*). Noticeably, the significant dissociations between the tail domain and the "pincer" formed by D1-D3 and between the constituent domains of the pincer occur in the temperature range near the midpoint ($T \approx 0.75$) of thermal denaturing curve of the whole vinculin (curve not shown). This observation indicates that the interactions between these domains contribute cooperatively to the stability of the whole vinculin.

As temperature increases, the dissociations between domains are followed by the significant unfolding of individual domains, suggesting that the thermal melting of vinculin occurs in a hierarchical manner. We observed a sigmoidal decrease in the fraction of intradomain native contacts ($Q_{\text{intradomain}}$) with increasing temperature (Fig. 2*b*). For each domain, at low temperatures most native contacts are kept and, thus, the $Q_{\text{intradomain}}$ is close to 1 ($Q_{\text{intradomain}} = 1$ in the fully folded state). At high temperatures most native contacts are disrupted, and the $Q_{\text{intradomain}}$ is $\sim$0 ($Q_{\text{intradomain}} = 0$ in the fully unfolded state). The midpoint of each curve is the folding transition temperature of the corresponding domain. We find that Vt domain shows higher stability than other domains, which is indicated by the relatively higher folding transition temperature (Fig. 2*b*). The remaining domains show different, but comparable, folding transition temperatures.

The Kinetics of Vinculin Unfolding—To better understand how external perturbations lead to the sequential disruption of interdomain interactions of vinculin, we performed kinetic unfolding of vinculin by gradually increasing the temperatures in the simulation. We collected and analyzed 20 kinetic unfolding simulation runs starting from the same native structure of vinculin but different initial velocities (see "Materials and Methods"). We found a specific sequential unfolding pattern across different unfolding trajectories (Figs. 3 and 4). Domains Vt and D3 are the first two domains that completely and irreversibly dissociate from each other, which is followed by Vt and D4 dissociation. Next, D1 and D2 dissociate. The native contacts

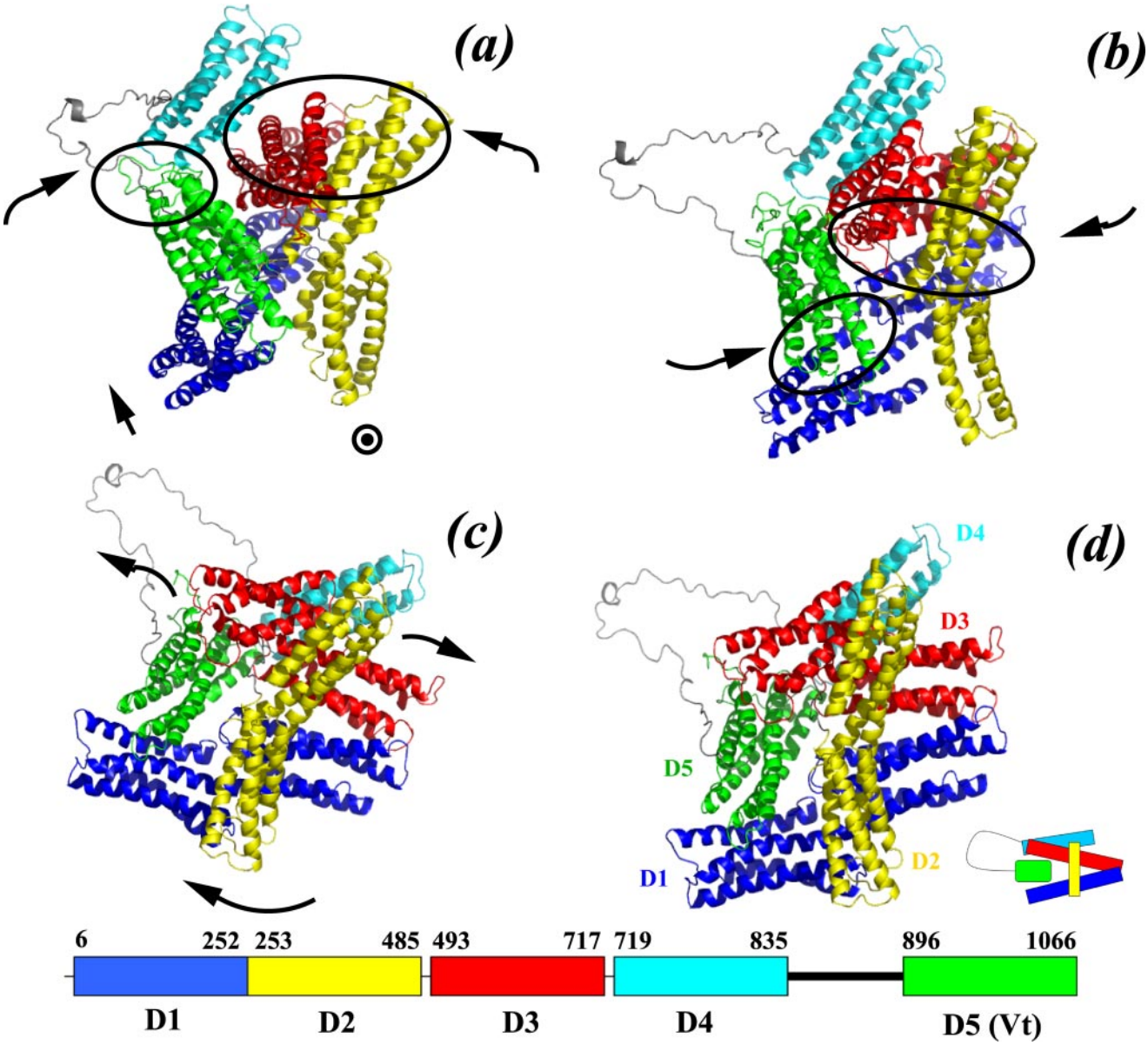

FIGURE 1. The native structure of full-length vinculin is shown in *d*. It is comprised of five distinct domains and one proline-rich linker region connecting the fourth and the fifth domain: D1, 6–252 (*blue*); D2, 253–485 (*yellow*); D3, 493–717(*red*); D4, 719–835 (cyan); the proline-rich linker region (838–890) consists of a proline-rich region (838–878) and a "strap" (878–890); D5 (vinculin tail), 896–1066 (*green*); the pincer-like structure formed between D1, D2, and D3 is illustrated at the *bottom right* beside the native structure. All the protein structures are made with PYMOL. The first three dominant modes of principal motions near the native state of vinculin are illustrated as follows: *a*, the first dominant mode; *b*, the second dominant mode; *c*, the third dominant mode.

between D1 and D2 were kept at a residual level ($Q_{\text{interdomain}} < 0.2$) due to oscillatory gain and loss of the local interactions between D1 and D2. Furthermore, a series of cooperative dissociations between domains D1-Vt, D2-D3, and D1-D3 (Fig. 4) occur. The dissociations between these domains occur close to each other in time, although in distinct temporal order in different simulations, suggesting a close interplay between these domains in response to the external perturbation through the unfolding process. Last, a marked decrease of native interactions between D3 and D4 occurs.

Accompanying the interdomain dissociations, the constituent domains start to unfold. Domains D1, D2, and D4 unfold first, followed by the unfolding of domains D3 and Vt (Fig. 4). Interestingly, the simulation reveals that the Vt domain unfolds via an intermediate state, whereas the unfolding of other domains exhibit apparent two-state behavior. Further structural characterization of the intermediate state of the Vt domain and the data from NMR experiments suggest its role in Vt function.[3]

The Role of Talin Binding in Vinculin Activation—The binding of talin to vinculin was postulated as an important mechanism for vinculin activation (15, 16, 33). It was proposed that the binding of talin to vinculin induces a conformational change of D1 domain of vinculin, which disrupts the interaction between D1 and Vt domains (15, 16, 33). However, most supporting evidence for this postulate was not obtained in the context of the whole vinculin. To shed light on the role of talin binding in activation of the whole vinculin, we studied the asso-

[3] R. D. Dixon, Y. Chen, N. V. Dokholyan, and S. L. Campbell, unpublished data.

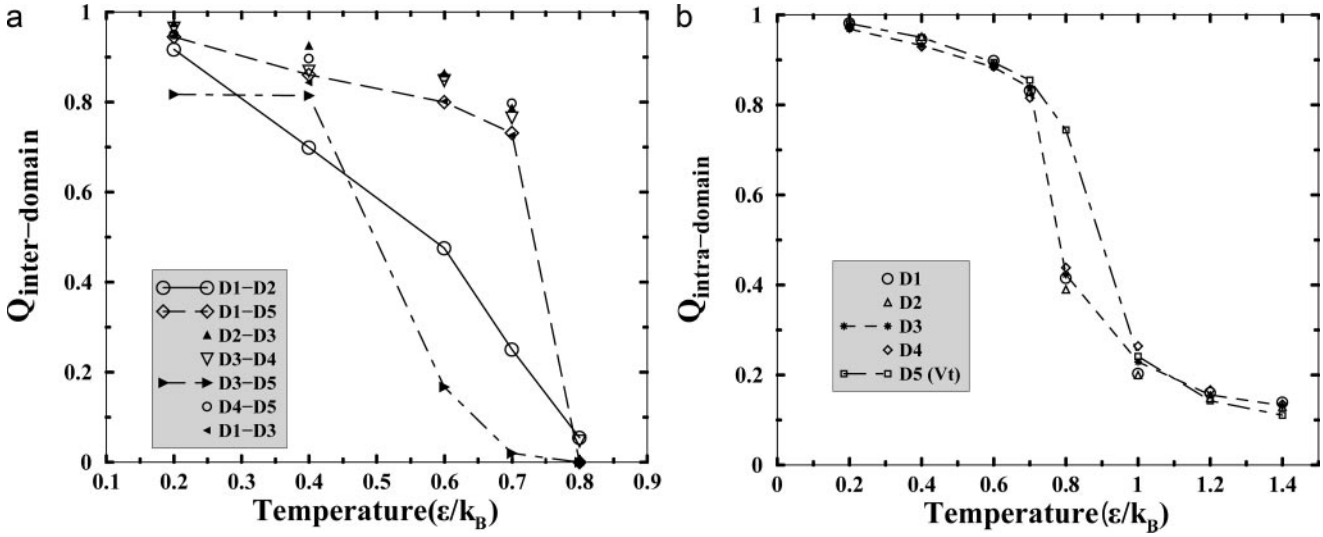

FIGURE 2. **The thermal melting curves of interdomain interactions (*a*) and intradomain interaction (*b*) are shown.** The magnitude of inter and intradomain dissociations are quantified using the fraction of native contacts made between ($Q_{interdomain}$) or within ($Q_{intradomain}$) domains. The *Q* values are calculated using trajectories from equilibrium simulations and plotted as a function of temperature. The higher the *Q* value, the smaller the magnitude of dissociation.

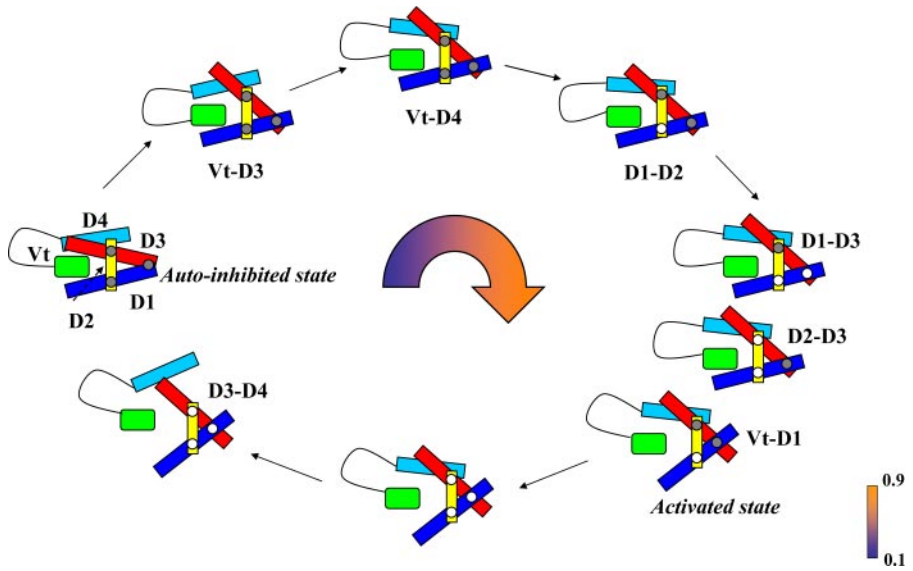

FIGURE 3. **A schematic representation is used to illustrate the sequential unfolding events in the kinetic simulations.** The five domains are colored as follows: *blue*, D1; *yellow*, D2; *red*, D3; *cyan*, D4; *black*, proline-rich linker region; *green*, Vt. The native contacts between domains in the pincer-like structure formed by D1-D3 are illustrated as *screws*. The loss of these native contacts is therefore represented as the taking-off of the screws. The unfolding events are connected by *arrows* with the increasing temperature and time along the direction of *arrows*. The labels near each unfolding event are the domain pairs that dissociate in the event. When several events occur close in time but not in a conserved temporal order, they are organized as one cluster without separations by *arrows*.

ciation of the vinculin-binding site (VBS1, residue 605–636) from talin and the full-length vinculin. We modeled the interaction between vinculin and VBS1 by an effective potential based on the crystal structure of D1-VBS1 complex (31) (see "Materials and Methods"). We performed DMD simulation of the binding of this peptide to vinculin at various temperatures. We found that the disruption of D1-Vt interaction occurs in a cooperative manner as was observed for the ligand-free state of vinculin. Interestingly, the temperature at which the D1-Vt interaction is completely disrupted is much lower in the presence of VBS1 ($T \approx 0.70$) than the ligand-free state of vinculin ($T \approx 0.76$), indicating that the binding of VBS1 peptide to vinculin significantly destabilizes the D1-Vt interaction (Fig. 5 and the legend therein). On the other hand, the binding of VBS1 peptide to vinculin is insufficient to disrupt D1-Vt interaction under native conditions (Fig. 5), suggesting a high free energy barrier between active and inactive state of vinculin in the presence of VBS1 in the simulation.

DISCUSSION

The Influence of Inherent Flexibility on Allostery of Vinculin—The ability to adopt distinct conformations upon the binding of diverse ligands makes vinculin a multifarious allosteric protein. We find that the intrinsic flexibility of vinculin, which is defined in the absence of ligand, has a large influence on the allosteric properties of vinculin. The two most dominant motions characterized in our simulation in the absence of any ligand binding differ in details, but they both involve "opening" and "closing" motions between Vt domain and structural elements of the pincer-like structure formed by D1, D3, and D2. These motions represent the intrinsic tendencies of the transitions between the closed, inactive state and an open state. The observed flexibility of vinculin is mainly determined by its native topology, suggesting that the native topology plays an important role in determining allosteric properties of vinculin.

Interestingly, it was found in recent studies (34) that the conformational changes of proteins upon ligand/protein binding are often well recapitulated by the intrinsic global motions of proteins in the unbounded state. These global motions are predominantly defined by native-contact topology of proteins (34).

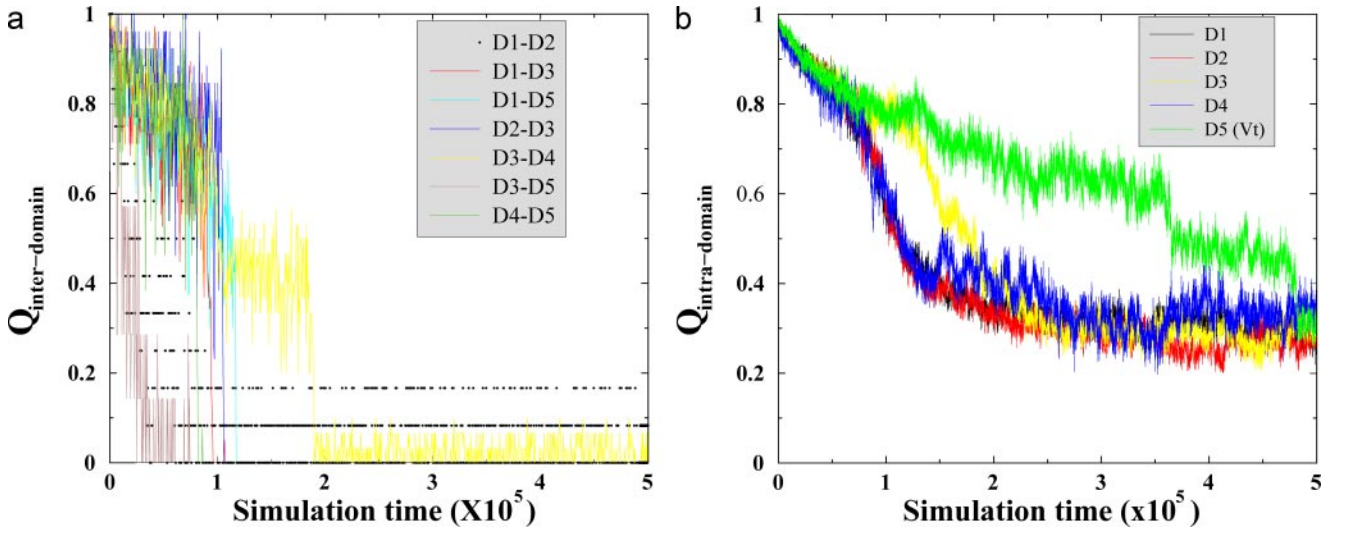

FIGURE 4. **A sample trajectory from kinetic unfolding simulations.** The fractions of native contacts between domains (*a*) and within domains (*b*) are plotted as a function of simulation time.

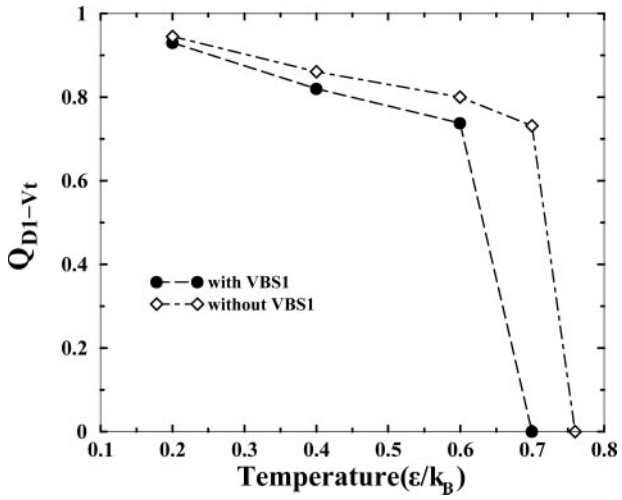

FIGURE 5. **The fraction of native contacts Q_{D1-Vt} made between D1 and Vt domains is plotted as a function of temperature.** The *Q* value is calculated using trajectories from equilibrium simulations of the whole vinculin in the presence of VBS1 (605–636) peptide from talin. The temperature at which D1-Vt interaction is completely disrupted ($Q = 0$) is around $T = 0.70$, while in the absence of VBS1, this temperature is around $T = 0.76$.

Hence, although the actual allosteric response is triggered by ligand binding, native topology may to a large extent define the plausible allostery of a protein.

The Cooperative Nature of Vinculin Activation Makes It an Allosteric Switch—Despite the observation that the intrinsic plasticities of vinculin largely define the conformational changes associated with vinculin activation, the interaction interface between D1 and Vt remains rigid in all the dominant modes of principal motions near the native state. Therefore, it is the ligand binding that is required for the disruption of D1-Vt interactions and vinculin acitivation. The current model of vinculin activation triggered by ligand binding is mainly based on two complementary lines of evidence. One comes from studies of the interaction between Vt and PtdIns(4,5)P_2 (12–14). As suggested in the limited proteolysis experiments (14), the binding of PtdIns(4,5)P_2 to Vt triggers a pronounced conformational change of Vt that in turn inhibits the D1-Vt interactions and exposes actin-binding and protein kinase C phosphorylation sites in Vt. The other line of evidence comes from more recent studies of the interaction between D1 and talin (15, 16, 35). Remarkably, the structures of D1 bound to talin peptides show that the first half of D1 converts from a four- to a five-helix bundle upon binding, with a simultaneous repacking of the hydrophobic core (16). It was hypothesized that this "helix bundle conversion" produces a conformation that is incompatible with the D1-Vt interaction interface that can in turn disrupt the D1-Vt interactions. Instead of directly competing for the Vt-binding surface of D1, talin alters the structure of D1. However, several other studies showed that larger fragments of talin bind poorly to full-length vinculin *in vitro* (11, 12). The addition of PtdIns(4,5)P2 is sufficient to increase the binding strength between talin and D1 4-fold (12). Hence, the role of talin binding in the activation of full vinculin activation remains controversial (17).

We find that the binding of VBS1 peptide from talin to vinculin does significantly destabilize the D1-Vt interaction. Also, the VBS1 binding is insufficient to completely disrupt the D1-Vt interaction under native conditions. The latter observation is not fully consistent with the recent experimental observations that the titration of VBSs from talin disrupts the D1-Vt interaction between the disjoined head and tail fragments of vinculin (complex formed between residues 1–840 and residues 879–1066) at room temperature (33). This result speaks to the possibility that our simulation may overestimate the free energy barrier between the active and inactive states of vinculin in the presence of VBS1. We speculate that the main factor leading to this overestimation is that the binding of VBS1 to the D1 domain in vinculin induces intermediate conformational changes stabilized by interactions that are absent in the final native D1-VBS1 structure, while the Gō potential used in our simulation (see "Materials and Methods") cannot capture those favorable interactions non-existent in the native structure. Therefore, a further characterization of these possible intermediate conformations in the kinetic experiments is of great interest.

We also observed a cooperative dissociation of between D1 and Vt in both thermodynamic and kinetic simulations with

increasing temperature, suggesting that vinculin activation may not be a stepwise, but rather a cooperative, process. Once the binding of the ligands is able to overcome the activation barrier, vinculin rapidly becomes activated. The cooperative nature of vinculin activation may give rise to the switch-like property of vinculin in integrating the external signals (the specific ligand binding).

Recently, two studies pointed out that vinculin may play important regulatory roles rather than merely being a structural link between the actin cytoskeleton and adhesion receptors (1, 36). First, it was found that the recruitment of the Arp2/3 complex to vinculin is required for efficient lamellipodial protrusion (1), suggesting that vinculin might couple cell adhesion and membrane protrusion by localizing actin assembly to sites of newly engaged integrins (1, 37). Second, vinculin regulates cell survival and migration by modulating the recruitment of paxillin to focal adhesions (36). Therefore, the switch-like property and the requirement of multiple ligand binding for activation enables vinculin to function as an "AND" logic switch in rapid response to the regulatory signals and exert dynamic control over downstream events.

The Synergistic Contribution from Domain-Domain Interactions to Vinculin Activation—The dissociations between Vt and D4 and Vt and D3 domains are two obligatory steps on the route to the disruption of the D1-Vt interaction in kinetic unfolding simulations. This observation suggests that besides the D1-Vt interaction, the direct interactions between Vt and other domains may also be essential in modulating vinculin activation. Consistent with our observation, Cohen *et al.* (38) recently provided compelling biochemical evidence that the interactions between Vt and D4 are important in maintaining the autoinhibited state of vinculin.

The dissociations between domains D1-Vt and the disassembly of the pincer-like structure (the dissociations between D2-D3 and D1-D3) occur in a cooperative manner (close to each other temporally) despite that the temporal order of the occurrence is not conserved. This observation raises a possibility that these domains may form a rigid cooperative unit, in which the significant dissociation between any pair of domains in this unit may subsequently trigger the dissociations between other domains upon even a slight external perturbation (such as ligand binding and temperature). Hence, we hypothesize that the disruption of D1-Vt interactions may involve a synergistic interplay between other domains. This hypothesis is experimentally testable as it predicts that the mutations weakening the interactions between D2 and D3 and D1 and D3 may effectively destabilize the autoinhibited state of vinculin.

Acknowledgments—We thank Dr. Sharon Campbell for helpful discussions. We also thank Dr. Richard Dixon and Kyle Wilcox for their help with the manuscript.

REFERENCES

1. DeMali, K. A., Barlow, C. A., and Burridge, K. (2002) *J. Cell Biol.* **159,** 881–891
2. Fernandez, J. L. R., Geiger, B., Salomon, D., Sabanay, I., Zoller, M., and Benzeev, A. (1992) *J. Cell Biol.* **119,** 427–438
3. Fernandez, J. L. R., Geiger, B., Salomon, D., and Benzeev, A. (1993) *J. Cell Biol.* **122,** 1285–1294
4. Volberg, T., Geiger, B., Kam, Z., Pankov, R., Simcha, I., Sabanay, H., Coll, J. L., Adamson, E., and Ben Ze'ev, A. (1995) *J. Cell Sci.* **108,** 2253–2260
5. Xu, W., Baribault, H., and Adamson, E. D. (1998) *Development* (*Camb.*) **125,** 327–337
6. Johnson, R. P., and Craig, S. W. (1995) *Nature* **373,** 261–264
7. Johnson, R. P., and Craig, S. W. (1995) *Biochem. Biophys. Res. Commun.* **210,** 159–164
8. Pokutta, S., and Weis, W. I. (2002) *Curr. Opin. Struct. Biol.* **12,** 255–262
9. Zamir, E., and Geiger, B. (2001) *J. Cell Sci.* **114,** 3583–3590
10. Critchley, D. R. (2000) *Curr. Opin. Cell Biol.* **12,** 133–139
11. Bakolitsa, C., Cohen, D. M., Bankston, L. A., Bobkov, A. A., Cadwell, G. W., Jennings, L., Critchley, D. R., Craig, S. W., and Liddington, R. C. (2004) *Nature* **430,** 583–586
12. Gilmore, A. P., and Burridge, K. (1996) *Nature* **381,** 531–535
13. Weekes, J., Barry, S. T., and Critchley, D. R. (1996) *Biochem. J.* **314,** 827–832
14. Bakolitsa, C., de Pereda, J. M., Bagshaw, C. R., Critchley, D. R., and Liddington, R. C. (1999) *Cell* **99,** 603–613
15. Izard, T., and Vonrhein, C. (2004) *J. Biol. Chem.* **279,** 27667–27678
16. Izard, T., Evans, G., Borgon, R. A., Rush, C. L., Bricogne, G., and Bois, P. R. J. (2004) *Nature* **427,** 171–175
17. Demali, K. A. (2004) *Trends Biochem. Sci.* **29,** 565–567
18. Dokholyan, N. V., Buldyrev, S. V., Stanley, H. E., and Shakhnovich, E. I. (1998) *Fold. Des.* **3,** 577–587
19. Rapaport, D. C. (2004) *The Art of Molecular Dynamics Stimulation*, 2nd Ed., pp. 391–417, Cambridge University Press, Cambridge, UK
20. Smith, S. W., Hall, C. K., and Freeman, B. D. (1997) *J. Comput. Phys.* **134,** 16–30
21. Sanchez, R., and Sali, A. (1997) *Curr. Opin. Struct. Biol.* **7,** 206–214
22. Berman, H. M., Westbrook, J., Feng, Z., Gilliland, G., Bhat, T. N., Weissig, H., Shindyalov, I. N., and Bourne, P. E. (2000) *Nucleic Acids Res.* **28,** 235–242
23. Ding, F., Prutzman, K. C., Campbell, S. L., and Dokholyan, N. V. (2006) *Structure* (*Camb.*) **14,** 5–14
24. Ding, F., Dokholyan, N. V., Buldyrev, S. V., Stanley, H. E., and Shakhnovich, E. I. (2002) *Biophys. J.* **83,** 3525–3532
25. Abe, H., and Go, N. (1981) *Biopolymers* **20,** 1013–1031
26. Go, N., and Abe, H. (1981) *Biopolymers* **20,** 991–1011
27. Ding, F., Dokholyan, N. V., Buldyrev, S. V., Stanley, H. E., and Shakhnovich, E. I. (2002) *J. Mol. Biol.* **324,** 851–857
28. Onuchic, J. N., Nymeyer, H., Garcia, A. E., Chahine, J., and Socci, N. D. (2000) *Adv. Protein Chem.* **53,** 87–152
29. Amadei, A., Linssen, A. B., and Berendsen, H. J. (1993) *Proteins* **17,** 412–425
30. Ichiye, T., and Karplus, M. (1991) *Proteins Struct. Funct. Genet.* **11,** 205–217
31. Papagrigoriou, E., Gingras, A. R., Barsukov, I. L., Bate, N., Fillingham, I. J., Patel, B., Frank, R., Ziegler, W. H., Roberts, G. C., Critchley, D. R., and Emsley, J. (2004) *EMBO J.* **23,** 2942–2951
32. Berendsen, H. J., and Hayward, S. (2000) *Curr. Opin. Struct. Biol.* **10,** 165–169
33. Bois, P. R., O'Hara, B. P., Nietlispach, D., Kirkpatrick, J., and Izard, T. (2006) *J. Biol. Chem.* **281,** 7228–7236
34. Tobi, D., and Bahar, I. (2005) *Proc. Natl. Acad. Sci. U. S. A.* **102,** 18908–18913
35. Bass, M. D., Smith, B. J., Prigent, S. A., and Critchley, D. R. (1999) *Biochem. J.* **341,** 257–263
36. Subauste, M. C., Pertz, O., Adamson, E. D., Turner, C. E., Junger, S., and Hahn, K. M. (2004) *J. Cell Biol.* **165,** 371–381
37. DeMali, K. A., and Burridge, K. (2003) *J. Cell Sci.* **116,** 2389–2397
38. Cohen, D. M., Chen, H., Johnson, R. P., Choudhury, B., and Craig, S. W. (2005) *J. Biol. Chem.* **280,** 17109–17117